

Electron transport in magnetic tunnel junctions

Dhavala Suri¹, R. S. Patel¹ and Abhiram Soori^{2,3}

1. *Department of Physics, Birla Institute of Technology and Science
Pilani - K K Birla Goa Campus, Zuarinagar, Goa 403 726, India.*

2. *International Centre for Theoretical Sciences (TIFR), 151, Shivakote, Bengaluru 560089, India.*

3. *Department of Physics, Indian Institute of Science, Bengaluru 560012, India.*

Magnetic tunnel junctions comprising of an insulator sandwiched between two ferromagnetic films are the simplest spintronic devices. Theoretically, these can be modeled by a metallic Hamiltonian in both the lattice and the continuum with an addition of Zeeman field. When mapped, the lattice and the continuum models show a discrepancy in the limit of a large Zeeman field. We resolve the discrepancy by modeling the continuum theory in an appropriate way.

I. INTRODUCTION

Magnetic tunnel junctions are basic building blocks of spintronic devices¹. The experiments by Moodera et.al and Miyazaki et.al^{2,3} (1995) on magnetic tunnel junctions demonstrated a large tunnel magnetoresistance (TMR) at room temperature and resulted in up-surge of activities in this field. Parkin et.al⁴ used MgO as a tunnel barrier and enhanced the TMR to nearly 200 %. A more recent experiment⁵ (2008) reported a much higher value of TMR at room temperature. Theoretically, magnetic tunnel junctions have been modeled even recently with the objective of studying the electron transport across the junctions⁶⁻⁹. In experimental systems, the junction can be tuned between ON and OFF states by an externally applied magnetic field^{2,5}. The ON state is when the spins in the two FM's are parallel and OFF state is when the two spins are anti-parallel. In the ON state, the current between the two FM's due to an applied bias is large and in the OFF state, it is small. However, theoretically the two FM's can be in a configuration that is more general than ON and OFF, where the spins in the two ferromagnets are aligned at a relative angle θ (with $0 \leq \theta \leq \pi$). We shall use this as a *theoretical tool* to understand the modeling of tunnel junctions. The experimental realizations generally correspond to the cases $\theta = 0$ (ON) and $\theta = \pi$ (OFF).

In Sec. II, we discuss the continuum and lattice models that describe a ferromagnet, followed by an outline of a mapping from continuum to lattice model. In Sec. III, we discuss the modeling of the tunnel junction. In Sec. IV, we calculate conductance. In Sec. V, we point to the discrepancy between the two models and resolve it. In Sec. VI, we summaries and end with concluding remarks.

II. MODELS OF FERROMAGNET

A. Continuum model

In continuum, a FM can be modeled by the Hamiltonian-

$$H_c = (\hbar^2 \vec{k}^2 / 2m - \mu_c + E_Z) \sigma_0 - E_Z \sigma_z, \quad (1)$$

where σ_i for $i = 0, x, y, z$ denote the Pauli spin matrices, the parameters m , μ_c , E_Z denote the effective mass of electrons, chemical potential and the Zeeman energy respectively. The dispersions for up- and down-spins are respectively given by $E_\uparrow = \hbar^2 \vec{k}^2 / 2m - \mu_c$ and $E_\downarrow = \hbar^2 \vec{k}^2 / 2m - \mu_c + 2E_Z$. By convention, Fermi energy is at zero and whenever a bias is applied, it is at the Fermi energy that the bias window $[-eV_0, +eV_0]$ is placed. It is easy to see that the band-bottom for up- and down- spins are at the energies $-\mu_c$ and $(2E_Z - \mu_c)$ respectively.

B. Lattice model

The ferromagnet can also be modeled by a lattice Hamiltonian on a cubic lattice-

$$H_l = \sum_{\vec{n}, \vec{e}} [-t(c_{\vec{n}+\vec{e}}^\dagger c_{\vec{n}} + c_{\vec{n}}^\dagger c_{\vec{n}+\vec{e}}) - (\mu_l - E_Z) c_{\vec{n}}^\dagger c_{\vec{n}} - E_Z c_{\vec{n}}^\dagger \sigma_z c_{\vec{n}}], \quad (2)$$

where $c_{\vec{n}} = [c_{\vec{n}, \uparrow}, c_{\vec{n}, \downarrow}]^T$ and $c_{\vec{n}, \sigma}$ is the second quantized annihilation operator for the spin- σ electron at site \vec{n} , and \vec{e} takes on unit vectors along x, y, z -directions. The parameters t , μ_l , E_Z are the hopping strength, chemical potential and the Zeeman energy respectively for the lattice model. In certain limits, these parameters can be mapped on to the parameters in the continuum model. The dispersion for the up-spin and the down-spin electrons in the lattice model take the form: $E_\uparrow = -2t[\cos(k_x a) + \cos(k_y a) + \cos(k_z a)] - \mu_l$ and $E_\downarrow = -2t[\cos(k_x a) + \cos(k_y a) + \cos(k_z a)] - \mu_l + 2E_Z$. The parameter a is the lattice spacing.

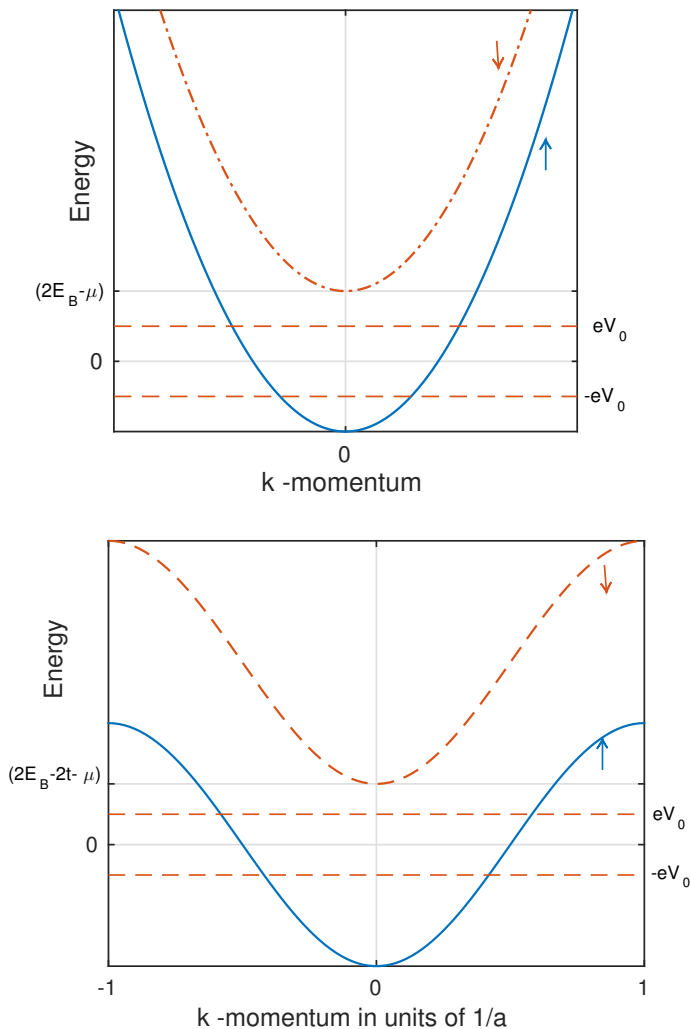


FIG. 1: Schematic of the dispersions for a ferromagnet modeled by continuum (on left) and lattice (on right) - Hamiltonians.

C. Mapping between the two models of ferromagnet

A schematic of the dispersions for the lattice and the continuum is shown in Fig. 1. We work in the range of parameters: (i) $0 < eV_0 < \min(\mu_c, 2E_Z - \mu_c)$ in the continuum and (ii) $0 < eV_0 < \mu_l < 6t$ and $eV_0 < (2E_Z - 6t - \mu_l)$ in the lattice. The dispersion relation for a continuum model is isotropic while that for the lattice model is not isotropic except very close to the band bottom. We now discuss on how to map from the continuum model to a lattice model. The lattice model is an effective model and may not depict the underlying lattice structure of the material, but agrees with the continuum model at low energies. Starting from a continuum model, we set the Zeeman energy in the lattice model to be the same (E_Z). The condition $\mu_l = \mu_c - 6t$ ensures that the band

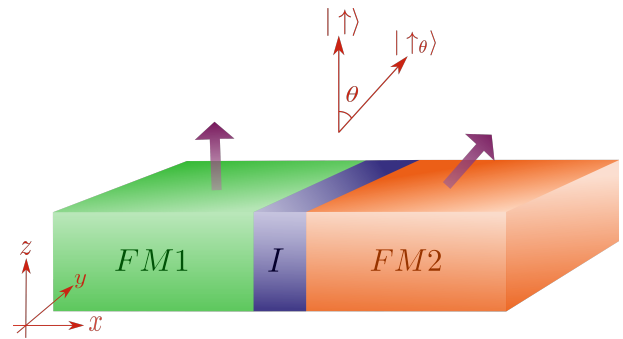


FIG. 2: Schematic of the setup under investigation. Two ferromagnets have their easy axes oriented at a relative angle θ . A thin insulator is sandwiched between the two ferromagnets.

bottoms of the two models are aligned. The lattice dispersion has the same form as in the continuum in the limit when $k_x a, k_y a, k_z a \ll \pi/2$, which can be seen by Taylor expanding the lattice dispersion around $\vec{k} = \vec{0}$ and keeping terms upto second order in $\vec{k}a$. This gives us: $ta^2 = \hbar^2/2m$. We choose the lattice constant a by demanding that in the bias window, the binomial expansion of the lattice dispersion is a good approximation: $a \ll \hbar\pi/2\sqrt{2m(\mu_c + eV_0)}$. Once a is chosen to satisfy the above condition, $t = \hbar^2/2ma^2$.

When E_Z is large enough so that $(2E_Z - \mu_c) > eV_0$ [same as $(2E_Z - \mu_l - 6t) > eV_0$], the down spin branch of the dispersion does not lie in the bias-window and the FM has 100% polarization with only up-spin channel being occupied at zero temperature. We call such a ferromagnet a “*pure FM*”. At a finite temperature, the down-spin channel has a small but finite occupation and the polarization is less than 100% in such *pure FM*s. The exact value of polarization at a given temperature depends on how large E_Z is and decreases monotonically with E_Z . We also introduce the limit $E_Z \rightarrow \infty$, in which we call the ferromagnet a “*perfect FM*” since the polarization even at a finite temperature remains at 100%.

III. JUNCTION BETWEEN TWO FERROMAGNETS

In continuum, a junction between two ferromagnets is typically described by respective Hamiltonians on either sides of $x = 0$ with boundary condition (BC) applied to the wavefunction at $x = 0$. A junction between FM’s pointing in two directions which are at angle θ is modeled when the Hamiltonian on left is given by Eq. (1) and the Hamiltonian on the right is given by Eq. (1), where σ_z is replaced by $\sigma_\theta = (\cos\theta \sigma_z + \sin\theta \sigma_x)$. The wavefunctions on either sides of the junction are equal and their derivatives differ by a quantity proportional to the

amplitude of the wavefunction at the junction-point:

$$\begin{aligned} \psi(x=0^+) &= \psi(x=0^-) \\ \partial_x \psi|_{x=0^+} - \partial_x \psi|_{x=0^-} &= q_0 \psi(x=0), \end{aligned} \quad (3)$$

where q_0 parametrizes the transparency of the junction. The limits $q_0 = 0$ and $|q_0| \gg \sqrt{2m\mu_c}/\hbar$ correspond to fully transparent and fully opaque junctions.

In the lattice model, the junction is typically characterized by a hopping t' between two sides of the lattices governed by different Hamiltonians and the BC does not appear. The information about the BC (of the continuum model) is carried by the hopping element t' in the \hat{x} -direction. The Hamiltonian on the left H_L is given by eq. (2) where $\vec{n} = (n_x, n_y, n_z)$ and n_x, n_y, n_z takes integer values such that $n_x \leq -1$. The Hamiltonian on the right H_R is given by eq. (2) where $\vec{n} = (n_x, n_y, n_z)$ and n_x, n_y, n_z take integer values such that $n_x \geq 0$, and σ_z replaced by $\sigma_\theta = (\cos \theta \sigma_z + \sin \theta \sigma_x)$ like in the continuum. The full Hamiltonian is:

$$\begin{aligned} H &= H_L + H_R + H_T, \quad \text{where} \\ H_T &= -t' \sum_{n_y, n_z} [c_{(1, n_y, n_z)}^\dagger c_{(0, n_y, n_z)} + h.c.], \end{aligned} \quad (4)$$

and n_y, n_z run over all integers.

We shall now specialize to the *perfect ferromagnet* limit, where $E_Z \rightarrow \infty$. Physically, this makes sense when the E_Z for the ferromagnet is much larger than all other energy scales in the problem. Also, this makes the calculations much simpler since one of the two spin channels is tends to be absent.

IV. TRANSPORT CALCULATIONS IN CONTINUUM AND LATTICE MODELS

We follow Landauer-Büttiker scattering approach^{11–15} to calculate conductance in continuum and lattice models. We write down a wavefunction which has incident and scattered parts and solve for the scattering coefficients. Since this is a three dimensional system, there are two angles of incidence and the total current at a given bias is calculated by integrating the currents over the full range of angles of incidence with appropriate factors. In the scattering theory calculation for tunnel junctions, an electron is incident at the junction and scattering amplitudes for scattering into different channels is calculated. Let α and β be the angles made by the incident electron having momentum $\vec{k} = (k_x, k_y, k_z)$ such that $\vec{k} = k(\cos \alpha, \sin \alpha \cos \beta, \sin \alpha \sin \beta)$. α is the angle made by the incident electron with x -axis, while β is the angle made by the projection of the momentum \vec{k} onto the (y, z) plane with y -axis. Due to translational invariance along \hat{y} - and \hat{z} - directions, the momenta k_y and k_z are good quantum numbers.

In continuum, the wavefunction of an electron incident on the tunnel junction at an energy E from left lead will

look like $e^{i(k_y y + k_z z)} |\psi(x)\rangle$ where,

$$\begin{aligned} |\psi(x)\rangle &= (e^{ik_x x} + r_{E,\alpha} e^{-ik_x x}) |\uparrow\rangle \quad \text{for } x < 0, \\ &= t_{E,\alpha} e^{ik_x x} |\uparrow_\theta\rangle \quad \text{for } x > 0, \end{aligned} \quad (5)$$

where $k_x = \sqrt{2m(\mu_c + E)} \cos \alpha / \hbar$ and the kets denote the spinors: $|\uparrow\rangle = [1, 0]^T$, $|\downarrow\rangle = [0, 1]^T$, $|\uparrow_\theta\rangle = [\cos(\theta/2), \sin(\theta/2)]^T$ and $|\downarrow_\theta\rangle = [-\sin(\theta/2), \cos(\theta/2)]^T$. Here, the wavevectors in the down-spin channels ($|\downarrow\rangle$ for $x < 0$, and $|\downarrow_\theta\rangle$ for $x > 0$) are absent since we have taken the limit of *pure ferromagnet*. To solve for the scattering amplitudes $r_{E,\alpha}$ and $t_{E,\alpha}$, we employ the boundary conditions discussed in Eq (3). It is easy to see from here that for any nonzero θ , $t_E = 0$ and hence the conductance of the junction is zero. This comes as a surprise. At $\theta = 0$, the problem becomes that of a spinless tunnel junction the conductance of which is dictated by the barrier strength q_0 .

In the lattice model, the wavefunction of an electron incident on the tunnel junction at an energy E from the left lead takes the form $|\psi\rangle = \sum_{n_x, n_y, n_z} e^{i(n_y k_y a + n_z k_z a)} |\psi_{n_x}\rangle |n_x, n_y, n_z\rangle$, where $|\psi_{n_x}\rangle = \psi_{n_x} \Theta[-n_x + 1] |\uparrow\rangle + \psi_{n_x} \Theta[n_x] |\uparrow_\theta\rangle$, where $\Theta[n_x]$ is discrete Heaviside step function and the kets retain the identity assigned in previous paragraph. This just states that electrons can point only along the easy axis and the easy axes of electrons on either sides of the junction differ by an angle θ . Further, the wavefunction takes the form:

$$\begin{aligned} \psi_{n_x} &= (e^{in_x k_x a} + r_{E,\alpha} e^{-in_x k_x a}), \quad \text{for } n_x \leq 0, \\ &= t_{E,\alpha} e^{in_x k_x a}, \quad \text{for } n_x \geq 1, \end{aligned} \quad (6)$$

where $k_x = \sqrt{2m(\mu_l + 6t + E)} \cos \alpha / \hbar$. We choose μ_l such that the lattice dispersion can be approximated to be a quadratic dispersion near the band bottom, as discussed in section II C. Note that μ_l so chosen is negative. The equation connecting the wavefunctions on either sides of the junction obtained from lattice Hamiltonian eq. (4), reduces to the following equations in the limit of *perfect ferromagnet*:

$$\begin{aligned} E_x \psi_0 &= -t\psi_{-1} - t' \cos(\theta/2)\psi_1 \\ E_x \psi_1 &= -t' \cos(\theta/2)\psi_0 - t\psi_2, \end{aligned} \quad (7)$$

where $E_x = (E + \mu_l + 6t) \cos^2 \alpha - 2t$. The term in eq. (7) proportional to t' can be understood as follows- since an $|\uparrow\rangle$ electron on site $n_x = 0$ does not flip spin while hopping on to $n_x = 1$, where the eigenspinor is $|\uparrow_\theta\rangle$, the overlap is $\langle \uparrow | \uparrow_\theta \rangle = \cos(\theta/2)$. Solving for the scattering amplitudes using eq. (7), we get

$$t_{E,\alpha} = \frac{-2i \sin(k_x a) t' \cos(\theta/2)}{[t^2 e^{-ik_x a} - t'^2 e^{ik_x a} \cos^2(\theta/2)]}, \quad (8)$$

and the differential conductance is given by

$$\begin{aligned} G &= G_0(E) \int_0^{\pi/2} d\alpha \sin \alpha \cos \alpha |t_{E,\alpha}|^2, \\ \text{where } G_0(E) &= \frac{e^2 m A (\mu_c + E)}{h \pi \hbar^2}, \end{aligned} \quad (9)$$

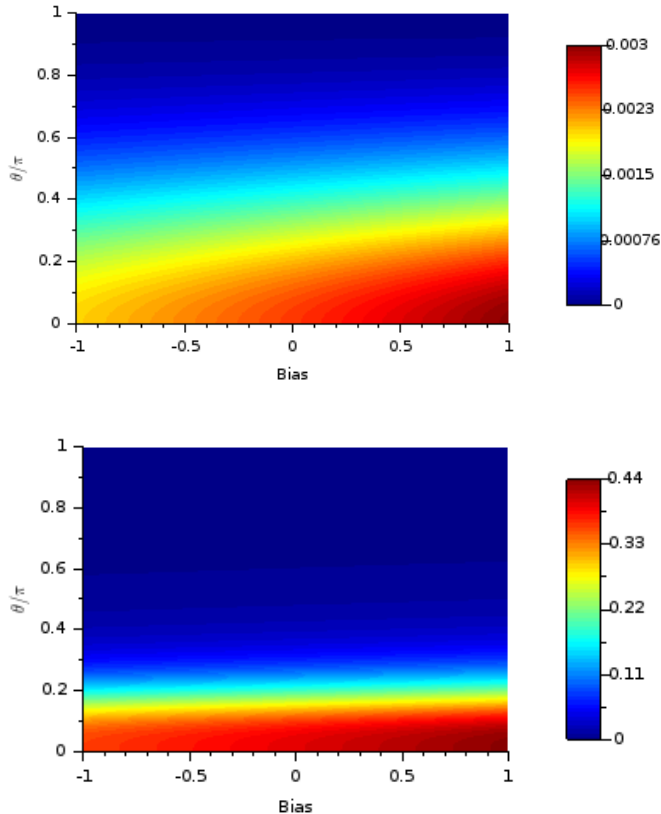


FIG. 3: Dependence of conductance in units of e^2/h on the bias and angle θ shown in contour plot for lattice model. Parameters: $t' = 0.535t$ for top and $t' = t$ for bottom, $\mu_l = -5.994 t$ for both.

and A is the area of cross section of the tunnel junction. The energy dependent factor $(\mu_c + E)$ in the conductance reflects the density of states in three dimensional ferromagnet. In Fig. 3, we show the result for differential conductance as a function of the angle θ and the bias.

V. DISCREPANCY AND ITS RESOLUTION

In the last section (sec. IV) we demonstrated that the lattice and the continuum models of the junction give highly distinct results for conductance of the magnetic tunnel junction made from *perfect FMs*. In the lattice model, the conductance is exactly zero only when $t' \cos(\theta/2) = 0$, while in the continuum model, the conductance is zero whenever $\theta \neq 0$. At this point, the results from lattice model look more reasonable. To resolve the puzzle, we now take lattice model as the starting point of analysis. The physical meaning of the hopping term H_T in the Hamiltonian [eq. (4)] is that the atomic wavefunctions on the two lattice sites when brought sufficiently close by overlap and the overlap is proportional

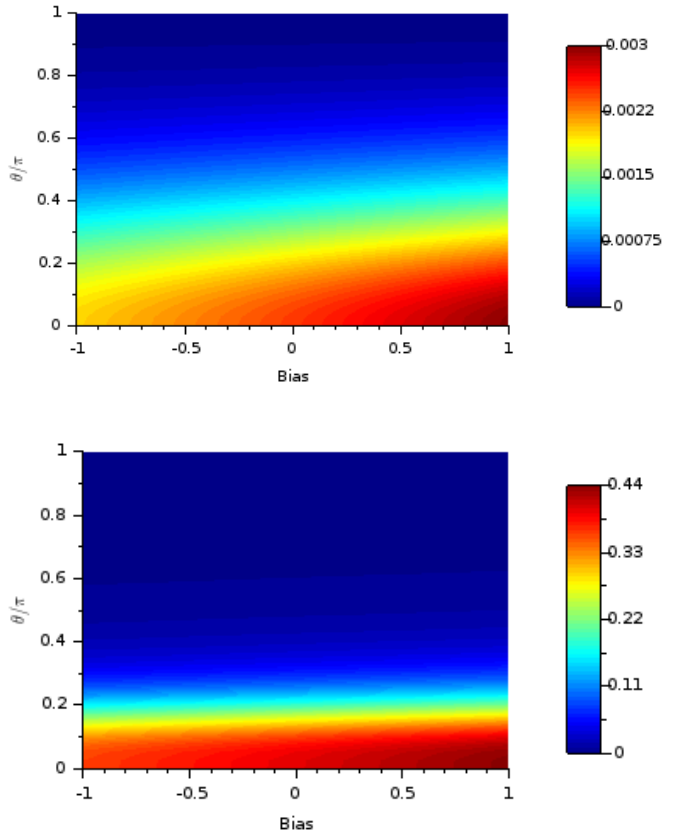


FIG. 4: Dependence of conductance in units of e^2/h on the bias and angle θ shown in contour plot for continuum model. Parameter $V_b = 2000$ for top and $V_b = 0$ for bottom. Other parameters have been mapped from lattice to the continuum as discussed in sec. II C: $m = 10$, $\mu_c = 10$, and $a = 0.0052952$.

to t' . In contrast, the wavefunctions on the two sides of the junction in the continuum model cannot overlap with each other whenever $\theta \neq 0$ since the limit $E_Z \rightarrow \infty$ does not allow any nonzero spin-component in a direction different from the easy axis. However, a region of finite length can be introduced between the two ferromagnets in the continuum model where both spin channels are allowed and the two wavefunctions can overlap. We show that introduction of such a region resolves the disagreement between the two models. The region in between can be modeled to have a length a and a barrier V_b that reflects the hopping element t' . The barrier V_b in the region $0 < x < a$ is isotropic in the spin space and the boundary conditions at $x = 0$ and $x = a$ are continuity of wavefunction ψ and its derivative $\partial_x \psi$. The limits $t' = t$ and $t' \rightarrow 0$ correspond to $V_b = 0$ and $V_b \rightarrow \infty$ respectively.

The wavefunction of an electron incident on the tunnel junction at an energy E from left lead will look like

$e^{i(k_y y + k_z z)} |\psi(x)\rangle$ where,

$$\begin{aligned} |\psi(x)\rangle &= (e^{ik_x x} + r_{E,\alpha} e^{-ik_x x}) |\uparrow\rangle \text{ for } x < 0, \\ &= \sum_{\sigma=\uparrow,\downarrow; \nu=+,-} s_{\nu,\sigma} e^{i\nu k'_x x} |\sigma\rangle \text{ for } 0 < x < a, \\ &= t_{E,\alpha} e^{ik_x x} |\uparrow_\theta\rangle \text{ for } x > a. \end{aligned} \quad (10)$$

Continuity of $|\psi(x)\rangle$ at $x = 0, a$ gives four equations while continuity of $\langle \uparrow | \partial_x |\psi(x)\rangle$ at $x = 0$ and continuity of $\langle \uparrow_\theta | \partial_x |\psi(x)\rangle$ at $x = a$ totally give six equations to be solved for six scattering amplitudes. We are interested in $t_{E,\alpha}$, since conductance can be calculated from it using eq. (9). We numerically compute $t_{E,\alpha}$ for each α , and integrate over α as shown in eq. (9) to get conductance for a given bias $E = eV$. The result for continuum model with a metallic (or insulating) layer in between the two FM's is presented in Fig. 4. The parameters for the two models have been chosen such that the final result looks the same and we have demonstrated this in the fully transparent and weakly transmitting limits. The results show a remarkable similarity both qualitatively and quantitatively.

VI. SUMMARY AND DISCUSSION

To summarize, we started with models of ferromagnets and using these as building blocks, studied magnetic tunnel junctions in both continuum and lattice models. In the limit of perfect FM, the discrepancy between the

continuum and the lattice models first came as a surprise. However, the results from the lattice model calculations appeared more convincing. We then resolved the discrepancy by appropriate modeling of the system in continuum model. The central result of our work is that magnetic tunnel junctions in the continuum model comprise of a nonmagnetic metallic (or insulating) layer sandwiched between the two ferromagnets. Absence of such a nonmagnetic region gives rise to unphysical results. However, in a lattice model, there is no need for a nonmagnetic layer for magnetic tunnel junction.

In this work we have primarily focused on perfect ferromagnets, where no modes in the direction other than spin easy axis is allowed. It will be interesting to investigate the lattice and continuum models in the pure ferromagnets where the wavefunction in the direction opposite to that of spin easy axis decays exponentially away from the junction. In junctions comprising of pure FM's, the nonmagnetic region may not be required in modeling since the wavefunctions opposite to spin easy axis can overlap in the region close to the junction. Further, connection to experimental systems is another future direction.

VII. ACKNOWLEDGEMENTS

We thank Diptiman Sen for stimulating discussions. DS thanks DST-INSPIRE, Govt. of India for PhD fellowship (No. DST/INSPIRE Fellowship/2013/742).

-
- ¹ I. Zutic, J. Fabian, and S. Das Sarma, "Spintronics: Fundamentals and applications", *Rev. Mod. Phys.* **76**, 323 (2004).
 - ² J. S. Moodera, L. R. Kinder, T. M. Wong, and R. Meservey, "Large Magnetoresistance at Room Temperature in Ferromagnetic Thin Film Tunnel Junctions", *Phys. Rev. Lett.* **74** 32733276 (1995).
 - ³ T. Miyazaki, N. Tezuka "Giant Magnetic Tunneling Effect in Fe/Al₂O₃/Fe Junction", *J. Magn. Magn. Mater.* **139**, L231 L234 (1995).
 - ⁴ S. S. P. Parkin, C. Kaiser, A. Panchula, P. M. Rice, B. Hughes, M. Samant and S.-H. Yang, "Giant tunnelling magnetoresistance at room temperature with MgO (100) tunnel barriers", *Nat. Mater.* **3**, 862 - 867 (2004).
 - ⁵ S. Ikeda, J. Hayakawa, Y. Ashizawa, Y.M. Lee, K. Miura, H. Hasegawa, M. Tsunoda, F. Matsukura and H. Ohno "Tunnel magnetoresistance of 604% at 300 K by suppression of Ta diffusion in CoFeB/MgO/CoFeB pseudo-spin-valves annealed at high temperature", *Appl. Phys. Lett.* **93** (8): 082508 (2008).
 - ⁶ K. Pasanai, "Similarities of coherent tunneling spectroscopy of ferromagnet/ferromagnet junction within two interface models: Delta potential and finite width model", *J. Magn. Magn. Mater.* **410**, 463-471 (2015).
 - ⁷ J. C. Slonczewski, J. Z. Sun, "Theory of voltage-driven current and torque in magnetic tunnel junctions", *J. Magn. Magn. Mater.* **310**, 169-175, (2007).
 - ⁸ Z-C. Wang, G. Su, Q-R. Zheng, and B-H. Zhao, "Spin tunneling in ferromagnet-insulator-ferromagnet junctions", *Phys. Lett. A* **277**, 47-55 (2000).
 - ⁹ Ph. Mavropoulos, N. Papanikolaou, and P. H. Dederichs, "Complex Band Structure and Tunneling through Ferromagnet /Insulator /Ferromagnet Junctions", *Phys. Rev. Lett.* **85**, 1088-1091 (2000).
 - ¹⁰ S. Datta and B. Das, "Electronic analog of the electrooptic modulator ", *Appl. Phys. Lett.* **56**, 665 (1990).
 - ¹¹ R. Landauer, "Spatial Variation of Currents and Fields Due to Localized Scatterers in Metallic Conduction", *IBM J. Res. Dev.* **1**, 223 (1957).
 - ¹² R. Landauer, "Electrical resistance of disordered one-dimensional lattices ", *Philos. Mag.* **21**, 863 (1970)
 - ¹³ M. Büttiker, Y. Imry, R. Landauer, and S. Pinhas, "Generalized many-channel conductance formula with application to small rings", *Phys. Rev. B* **31**, 6207 (1985)
 - ¹⁴ M. Büttiker, "Four-Terminal Phase-Coherent Conductance", *Phys. Rev. Lett.* **57**, 1761 (1986)
 - ¹⁵ S. Datta, *Electronic Transport in Mesoscopic Systems* (Cambridge University Press, Cambridge, 1995).